Very High Energy Gamma Ray Astronomy using HAGAR Telescope System

Varsha Chitnis (for HAGAR collaboration)
Department of High Energy Physics, Tata Institute of Fundamental Research, Homi Bhabha Road, Mumbai-400005, India
vchitnis@tifr.res.in

Very High Energy gamma ray astronomy is passing through a very exciting phase at present. This, comparatively new branch of astronomy has emerged as a major astronomical discipline during last decade, with the detection of more than 170 objects belonging to diverse astronomical classes. In this talk, a brief review of the field will be given. India has a long tradition of research in this area. At present 7-element High Altitude Gamma Ray (HAGAR) telescope system is operational in Ladakh region of Himalayas. This telescope system, the first phase of 4-Institute collaboration, Himalayan Gamma Ray Observatory (HiGRO), has been observing various astronomical sources since 2008 and has successfully detected VHE gamma ray emission from extragalactic objects like Mrk 421, Mrk 501 as well as galactic sources including Crab nebula/pulsar. Details of HAGAR telescope system will be given and some of the recent results as well as future plans will be discussed.

1. Introduction

Very High Energy or VHE gamma ray astronomy covering the energy range of few 10's of GeV - few 10's of TeV is one of the youngest branches of astronomy. It has evolved into a mature branch of astronomy during last decade, with the detection of more than 170 astronomical sources belonging to diverse classes. In the next section of this paper, brief review of the field is given. This is followed by description of HAGAR telescope system operational in Ladakh region of Himalayas for last few years and some of the recent resulted from HAGAR and future plans.

2. Physics motivation for VHE gamma ray astronomy

Gamma rays provide one of the best windows to study nonthermal universe. Cosmic rays with energies extending upto 10^{20} eV, following powerlaw distribution, form one nonthermal component. Even after more than 100 years since discovery, origin and acceleration of cosmic rays is unresolved mystery. Supernova remnants (SNRs) are thought to be the sites for lower energy cosmic rays upto 10^{15} eV i.e. upto the knee region of cosmic ray spectrum. Higher energy cosmic rays probably originate from Active Galactic Nuclei or AGNs. Acceleration of charged particles to very high energies produces gamma rays through various processes. So study of VHE gamma ray emission from these sources will shed some light on cosmic ray origin. This study will also give insight into emission regions and emission processes in these objects.

There are some other research areas which can be explored through study of VHE gamma ray emission. It is possible to study physics beyond standard model through searches for dark matter. WIMPs or weakly interacting massive particles are popular candidates for dark matter. Annihilation of WIMPs is expected to produce detectable signal in VHE gamma ray range. Likely candidate sites are galactic halo, galactic centre, dwarf galaxies or galaxy clusters.

There is also possibility to check for Lorentz invariance through study of rapid time variations in VHE emission from distant objects. Also it is possible to get indirect estimation of Extragalactic Background Light (EBL) through study of VHE emission from AGNs. This has implications about star formation history of the Universe.

VHE gamma ray emission has been detected from 175 sources so far [1]. These include variety of galactic and extragalactic objects. Amongst galactic sources prominent classes are supernova remnants (13 shell type SNRs and 10 with molecular clouds detected so far), pulsar wind nebulae or PWN (35), pulsars (2) and binaries (5). Amongst extragalactic sources these are predominantly AGNs (61), radio galaxies (4), starburst galaxies (2), massive star clusters (4) etc. Examples from some of the categories are discussed below.

2.1 Supernova remnants

Massive stars end their life through supernova explosions. This explosion blows off outer layers of star forming supernova remnant. Supernova remnants are thought to be the sites for acceleration of cosmic rays and possible mechanism is diffusive shock acceleration. VHE gamma ray emission from supernova remnants extending beyond few 10's of TeV provide indication of possible cosmic ray acceleration. VHE emission is detected from 13 shell type supernova remnants and 10 supernova remnants with molecular clouds. One example is supernova remnant RXJ1713.7-3946 detected by HESS with spectrum extending upto 100 TeV with slope of -2, which is consistent with shock acceleration scenario [2]. This is still not considered as conclusive evidence as these gamma rays could originate from neutral pion decay from proton proton interaction or by Compton scattering of VHE electrons with cosmic microwave background radiation. Present data is not able to distinguish between these two scenarios. Multiwaveband morphological studies with better angular resolution and spatially resolved spectral measurements are needed to settle this issue.

2.2 Pulsar wind nebulae (plerions)

In many cases supernova explosion results in rapidly rotating neutron star which is called pulsar. Quite often supernova remnants show bright core within the shell, powered by pulsar wind consisting of electrons and positrons. VHE gamma ray emission is detected from 35 PWN so far. One typical example is Crab nebula with nonthermal emission extending over 21 decades of frequencies. Spectral energy distribution (SED) of Crab nebula in gamma ray band is explained in terms of Synchrotron Self-Compton (SSC) model [3]. According to this model, relativistic electrons emit Synchrotron photons which are Compton upscattered to gamma ray energies by same population of electrons. Even though Crab nebula is a well studied object, there are several aspects which are not yet understood. For example, there were rapid high energy gamma ray flares with rise time of few hours seen by AGILE and Fermi-LAT, which are not yet fully understood [4].

2.3 Gamma ray pulsars

Pulsars are highly magnetized rapidly rotating neutrons stars where rotation axis is misaligned with magnetic field axis. As neutron star spins, the beam of radiation sweeps through our line of sight and we see pulsations. Pulsations are seen in various wavebands. Emission mechanism for gamma rays was thought to be curvature radiation produced when high energy charged particle moves along curved magnetic field, resulting in exponentially cutoff powerlaw spectrum. Exact shape of the spectrum depends on the place from where gamma ray emission originated. There are various models about the emission region like polar cap, outer gap and slot-gap etc.

VHE gamma ray pulsations were detected from Crab pulsar at a period of 33 ms initially by MAGIC telescope at energies above 25 GeV and later by VERITAS at energies above 100 GeV, upto 400 GeV [5]. Earlier gamma ray spectrum detected by Fermi-LAT was fitted with a exponential cutoff powerlaw consistent with curvature radiation. However, detection of pulsations at energies above 100 GeV cannot be explained by curvature radiation. Entire gamma ray spectrum is fitted with a broken power law and inverse Compton scattering is one likely mechanism. Also possibility of two mechanisms one dominant at lower gamma ray energies below the spectral break and second one dominant above the break is being discussed. Very recently MAGIC has detected pulsations from Crab pulsar all the way upto 1.5 TeV [6], further strengthening these interpretations.

Only other pulsar detected at VHE energies is Vela pulsar. This was detected by second phase of HESS, 28 m diameter telescope, i.e. the largest VHE gamma ray telescope in the world. Pulsations are seen clearly at a period of 89 ms at energies above 30 GeV [7].

2.4 TeV binaries

TeV binaries are composed of a massive star and a compact object and emit variable, modulated VHE emission. Five binaries are detected at VHE energies. One example is LSI+61° 303, where emission was found to show modulation of 26.5 days which is orbital period of the system. Companion star is Be star with circumstellar disk and nature of compact object, whether it is neutron star or black hole is not clear. VHE emission is mainly seen in the orbital phases of 0.4–0.7 [8]. There are two types of models proposed to explain this emission. According to

microquasar model, compact object is powered by mass accretion from companion star producing collimated jets. These jets boost energy of stellar photons to VHE gamma rays. According to binary pulsar scenario, pulsar winds are powered by rotation of neutron star and interaction of pulsar wind with companion star outflow produces VHE gamma rays [9]. It is not yet clear which model is correct. Multiwaveband studies are expected to provide the clue.

2.5 Active Galactic Nuclei

AGNs are the distant galaxies with bright nuclei, powered by supermassive black hole at the centre accreting matter from host galaxy. VHE gamma ray emission is detected from 61 Blazar classs AGNs including BL Lacs and FSRQs. Blazars are characterised by variability in all wavebands on various time scales ranging from minutes to years, with wide flux variations. These objects have jets pointed towards us, so we see Doppler boosted emission from jets. SEDs of these objects are characterised by two broad peaks or humps and depending on location of these peaks, Blazars are classified as Low-frequency peaked Blazars (LBL), Intermediate-frequency peaked Blazars (IBL) and High-frequency peaked Blazars (HBL). Most of the Blazars detected at VHE energies are HBL type. HBLs show first peak in SED at X-ray energies and second one at TeV energies. First peak is generally attributed to Synchrotron emission from energetic electrons, whereas origin of second peak is not clear. According to various proposed theories this emission could be originating from leptonic beam or hadronic beam in jets. One popular leptonic model is SSC model which readily explains good correlation seen between X-ray and gamma ray flares from several TeV Blazars. However, sometimes orphan TeV flares are also seen from some Blazars which not accompanied by corresponding increase at X-ray energies. These are inconsistent with SSC model and explained using other leptonic models like external Compton (EC) or hadronic models or lepto-hadronic models. EC model is similar to SSC but here photons for Compton upscattering come from elsewhere, from outside the jet, possibly from accretion disk, torus or BLR. This model is used quite often to explain gamma ray emission from LBLs and FSRQs. Amongst hadronic models there are proton synchrotron, proton induced cascades due to interaction of protons with ambient matter or photon fields. There is a particular interest in hadronic models from the point of view of explaining cosmic ray origin.

One important characteristic of Blazars is their time variability. This variability is seen in all wavebands including gamma ray band. One example is spectacular flare detected by HESS experiment from PKS2155-304, where flux increased as high as 15 Crab units with rise time of 173 s [10]. Another interesting flare was detected from Mkn 501 by MAGIC experiment lasting for about half an hour showing significant lag between photons of different energies in TeV band. Time delay of about 4 minutes was seen between lowest and highest energies in this case [11]. Using these kind of time lags, it is possible to constrain quantum gravity models. Using this particular flare, lower limits on quantum gravity parameter were derived. Another important information obtained from variability time scale is the size of the emission region.

One more important aspect of these studies is estimation of Extragalactic Background Light or EBL. EBL is isotropic diffuse radiation of UV, optical and IR photons. It is sum of starlight emitted by galaxies through the history of the Universe. EBL shows two humped spectral energy distribution. First hump in UV-optical corresponds to starlight and second hump corresponds to UV/optical light absorbed by dust and re-radiated in the infrared. Direct measurements of EBL are extremely difficult due to strong foreground contamination by galactic and zodiacal light. Various theoretical models are available, but these are poorly constrained. VHE gamma rays from distant AGNs interact with EBL photons producing electron positron pair resulting in distortion and attenuation of intrinsic spectrum. Attenuation depends on energy as well as distance of the source, generating gamma ray horizon. Distortion caused in VHE spectrum of Blazars by EBL can be used for estimation of EBL itself. One such attempt of evaluation of EBL was done using data from two Blazars at redshifts of 0.186 and 0.165 obtained from HESS experiment [12]. Upper limit on EBL derived from these measurements indicated that Universe is transparent than expected. This work was later extended using sample from seven Blazars and EBL was estimated over the wavelength range of 0.3-10 μm [13]. As more data becomes available these estimates will get revised further.

3. HAGAR Telescope System

3.1 Atmospheric Cherenkov Technique

Gamma rays from astronomical sources can not penetrate Earth's atmosphere and hence are detected using satellite based detectors. At energies above 100 GeV, due to rapidly falling flux from astronomical sources, it is not possible to use satellite based detectors very efficiently because of requirement for very large detector areas. On the other hand, VHE gamma rays are detected far more efficiently using ground based atmospheric Cherenkov technique. Gamma rays are detected indirectly in this technique. Gamma ray interacts at the top of the atmosphere, through various processes generates shower of charged particles in the atmosphere, these charged particles then cause atmosphere to emit bluish Cherenkov light (see Fig.1). This light is detected using telescope consisting of mirror/reflector and one or more photomultiplier tubes or PMTs at focus. This light comes as a flash lasting for a few ns and is spread over a circular region with radius of about 100 m at observation level. There are two variants of atmospheric Cherenkov technique, angular imaging and wavefront sampling. In imaging technique, there is a large reflector with cluster of PMTs at the focus. Images of air showers are recorded in this technique. On the other hand, in wavefront sampling technique, there is a distributed array of small size telescopes sampling Cherenkov light across the Cherenkov pool. In this technique, arrival time of Cherenkov shower front and Cherenkov photon density are recorded at various locations in Cherenkov pool. Arrival time information gives the direction of shower axis and Cherenkov photon density is a measure of primary energy. HAGAR telescope system is based on this technique.

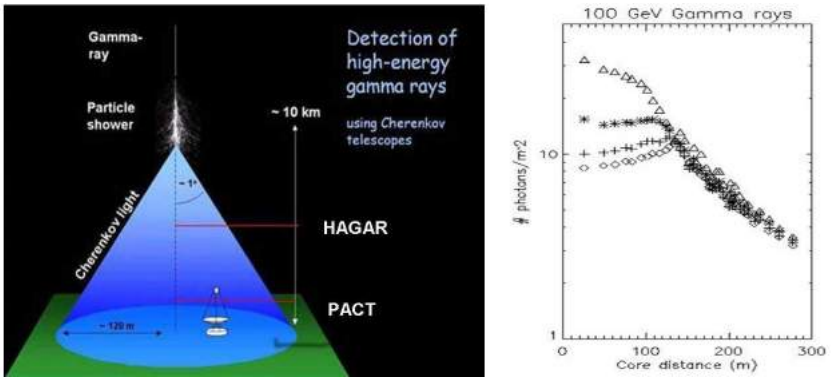

Figure 1. Left panel : Atmospheric Cherenkov technique, Right panel: Variation of Cherenkov photon density with core distance for simulated showers initiated by 100 GeV gamma rays for various altitudes (diamond : sea level, plus sign : 1 km, asterisk : 2.2 kms and triangle : 4.5 kms altitude)

3.2 HiGRO collaboration experiments

Tata Institute of Fundamental Research (TIFR) entered the field of VHE gamma ray astronomy in 1969. Initial activities were at Ooty and were shifted to Pachmarhi in Madhya Pradesh in 1980s. Bhabha Atomic Research Centre (BARC) also started activities in this field in 1980s. Recently TIFR was operating Pachmarhi Array of Cherenkov Telescopes and BARC has been operating TACTIC at Mt. Abu. Both these experiments are at an altitude of about 1 km and have low energy thresholds in the neighbourhood of about 1 TeV. There is a strong physics motivation for lowering energy thresholds of atmospheric Cherenkov telescopes. For example, detection of distant AGNs or GRBs and detection of pulsed component in pulsars is possible only with instruments with thresholds around 100 GeV or less. There are two ways of reducing energy threshold. First alternative is to use large mirrors, which is expensive. Second cost effective alternative is to install telescope at high altitude location. As one goes to high altitude location, Cherenkov photon density in the cone increases. Also atmospheric attenuation of Cherenkov photons is lower at high altitude locations. Because of these two factors, there is a significant increase in Cherenkov photon density near shower core at high altitude location. This is seen clearly from Fig.1 (right panel), where variation of Cherenkov photon density from simulated showers initiated by 100 GeV gamma rays is plotted as a function of distance from shower axis (or core distance) for four different altitudes

from sea level to 4.5 kms altitude. Cherenkov photon density near shower core is factor of 4-5 higher at 4.5 kms altitude than that at sea level. As a result, there is a significant reduction in energy threshold of atmospheric Cherenkov telescope installed at high altitude location.

Himalayan Gamma Ray Observatory (HiGRO) collaboration was formed with the motivation of setting up atmospheric Cherenkov telescopes at high altitude location in Himalayas. This is a collaboration between four institutes : TIFR, IIA (Indian Institute of Astrophysics), BARC and SINP (Saha Institute of Nuclear Physics). There is also some participation from Dibrugarh University in this collaboration. HiGRO experiments are located at a place called Hanle in Ladakh region of Himalayas. This is the place where IIA has set up Indian Astronomical Observatory (IAO). Altitude of the base camp of IAO is 4.3 kms. Ladakh is a high altitude cold desert with hardly any rainfall and very little snowfall with clear sky almost throughout the year. Hanle is easily accessible by road from Leh throughout the year at a distance of about 250 kms. HAGAR is the first phase of HiGRO and MACE, described in the paper [14], is the second phase.

3.3 HAGAR : instrument details

HAGAR or High Altitude Gamma Ray Telescope system is an array of seven telescopes deployed in the form of a hexagon (see Fig.2). Spacing between the telescopes is 50 m. Each telescope consists of seven para-axially mounted parabolic mirrors, each of diameter 0.9 m. At the focus of each mirror UV sensitive PMT from Photonis with make XP2268B is mounted. Field of view of HAGAR is 3 deg FWHM. Pulses from PMTs are brought to the control room through coaxial cables.

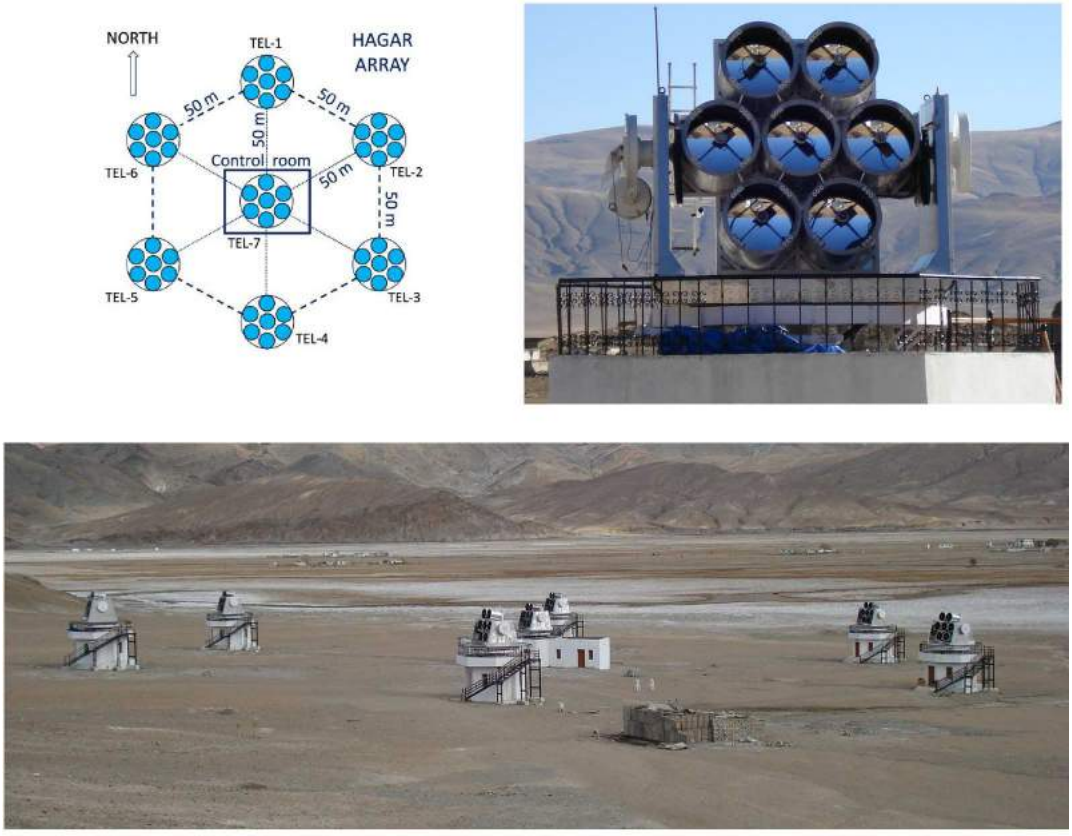

Figure 2. Top left : Layout for HAGAR, Top right : One of the telescopes from HAGAR, Bottom : HAGAR array of 7 telescopes

Installation of HAGAR began at Hanle in 2005 and was completed in 2008. Fig.2 shows the photograph of entire

array with closer view of one of the telescopes. Tracking system of HAGAR is based on alt-azimuth design. Maximum zenith angle coverage is upto 85 deg. Steady state pointing accuracy of servo is $\pm$10 arc-sec. Maximum slew rate is 30 deg/minute. Average pointing accuracy of a mirror is estimated to be 12.5 arc-minutes [15].

High voltages of individual PMTs of HAGAR are controlled using CAEN controller. In control room pulses from individual PMTs are added to form seven telescope pulses. Data acquisition system is CAMAC based and interrupt driven. Trigger is generated when at least 4 telescope pulses out of 7 cross the discriminator threshold in coincidence window of 60 ns. Data recorded for each event includes relative arrival time of shower front at each mirror accurate to 0.25 ns as given by TDCs, pulse height or charge at each telescope recorded using 12 bit ADC and absolute arrival time of event accurate to μs as given by Real Time Clock (RTC) module synchronised with GPS. In addition to this telescope pulse profiles are also recorded in 1 ns bins using waveform digitizer. Further details for HAGAR are given in [16].

3.4 Performance parameters for HAGAR

Extensive simulations were carried out to understand performance of HAGAR. Since atmospheric Cherenkov experiments cannot be directly calibrated, their performance can be understood only through simulations. These simulations consist of two parts. First part is the simulation of extensive air showers initiated by gamma rays and various species of cosmic rays. CORSIKA package is used for this purpose [17]. Packages GHEISHA and VENUS were used respectively for simulating low and high energy hadronic interactions whereas EGS4 was used for electron-photon interactions. US standard atmospheric profile was used. Showers initiated by gamma rays, protons, alpha particles and electrons were simulated. Impact parameter range was varied over 0-300 m, viewcone range of 0-4 deg was used for cosmic ray showers. HAGAR geometry and geomagnetic field at Hanle was taken into consideration. Mirror reflectivity was set to 80% and quantum efficiency curve for PMT was used. Typically few million showers were generated for each species. This sample was then passed through detector simulation program which takes into account various parameters specific to HAGAR system like PMT and cable response, trigger criteria etc. Further details of these simulations are given in [18].

Cosmic ray trigger rate estimated from these simulations is 13 Hz which agrees with the observed trigger rate. Energy threshold given as the peak of the differential rate curve is estimated to be about 208 GeV for 4 fold trigger condition. Expected gamma ray rate from Crab like sources is 6.3 counts per minute. Sensitivity corresponds to detection at the level of 1.2 $\sigma/\sqrt{hour}$ for Crab like sources. In other words, Crab nebula can be detected at a significance level of 5 sigma in 17 hours.

3.5 HAGAR observations and results

Regular observational runs with HAGAR commenced in September 2008. During last seven years more than 4000 hours of data were collected in the form of observational and various calibration runs. Observations of astronomical sources are typically carried out in ON-OFF pairs of duration about an hour each. Several galactic and extragalactic sources were observed in last seven years. Amongst galactic sources, the longest coverage is for Crab nebula/pulsar (about 320 hours) followed by Geminga pulsar (about 200 hours), whereas amongst extragalactic sources, longest coverage is for Mkn 421 (about 260 hours) followed by Mkn 501 (about 185 hours) and 1ES2344+514 (about 145 hours).

In data analysis, initially selection cuts based on data quality, stability of rates etc. are applied to data constituting ON-OFF pair. Then for each event, arrival direction of shower is determined. For this purpose, relative arrival times of shower front at various telescopes are fitted with a plane front. Normal to this front gives direction of shower axis. Then space angle, i.e angle between shower axis direction and pointing direction of the telescope is calculated. Space angle distributions generated for ON-OFF pairs are then compared and normalized and gamma ray signal is estimated as excess events in signal region. Some of the prominent results from HAGAR are given below.

3.5.1 *Crab nebula*

Crab nebula is a very well studied object discussed earlier. It is a bright and steady source considered as a standard candle. With HAGAR we had very long coverage for this source. After applying data quality cuts, 103 hours of data were left which were analysed further. Seasonwise count rates from Crab nebula for six years data are shown in Fig.3. Flux is estimated to be $(2.01 \pm 0.11) \times 10^{-10}$ ph/cm^2/s for the threshold of 234 GeV, which is consistent with the measurements from other experiments like Whipple and MAGIC (see Fig.3) [19].

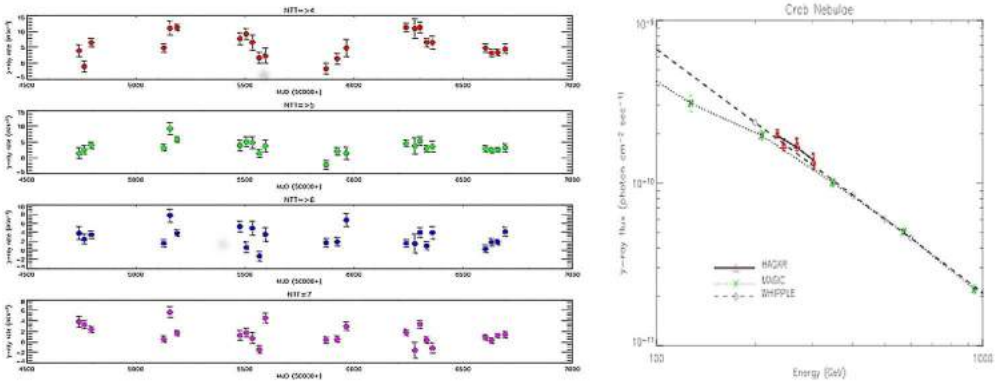

Figure 3. Left : Seasonal light curve of Crab nebula from HAGAR spanning six years of data. Different panels correspond to different trigger conditions, at least 4, 5, 6 and 7 telescopes triggering, from top to bottom. Right : Flux measurements from HAGAR as a function of energy shown by red triangles. Dotted and dashed lines correspond to spectral measurements from MAGIC and Whipple respectively.

3.5.2 *Crab and other pulsars*

Search for pulsations was carried out in Crab data collected by HAGAR. Data stretch of about 140 hours was used for this purpose. Using absolute arrival time of each event recorded with μs accuracy and using known ephemeris of pulsar with period of 33 ms, phase was calculated for each event and phasogram was generated which is shown in Fig.4. Excess is seen clearly at phases marked P1 and P2. These are the phases at which excess is seen by Fermi-LAT and other experiments. This type of excess is not seen in the background data validating the result. Significance of this excess is estimated. So there is indication of pulsations from Crab at significance level of 3.6σ [20]. Attempts are being made to improve the significance by adding more data and also by refining the cuts applied in analysis. Some more pulsars including Geminga, PSR J0357+3206, PSR J0633+0632 and PSR J2055+2539 were observed with HAGAR. There is no statistically significant detection of pulsations from any of these pulsars and upper limits on pulsed flux are estimated.

3.5.3 *Mkn 421*

Amongst extragalactic sources, we had longest coverage for Mkn 421. This is a nearby Blazar (z=0.031) of HBL type. VHE gamma ray emission was discovered by Whipple from this source in 1992. This was the first blazar to be detected at VHE gamma ray energies. It is known to show frequent flaring behaviour. One large flare from this source appeared in February 2010, which was seen by VERITAS, HESS and HAGAR. Results from HAGAR data collected during February-April 2010 are shown in Fig.5. This figure shows seasonwise count rates from HAGAR for estimated energy threshold of 250 GeV. In February, from 8 hours of data, source was detected at the significance level of 12.7σ. Mean count rate was 13.4 counts per minute and rate decreased in subsequent seasons. Fig.6 shows lightcurve from HAGAR along with the X-ray light curve from ASM onboard RXTE. Similar pattern is seen in both the cases. HAGAR detected maximum flux on the night of 17th February and flux level was about 6-7 crab units. Average flux in February was 3 crab units and it decreased to one crab unit in March and April.

Fig.6 shows multiwaveband data for February 2010 flare. These data were obtained from following instruments,

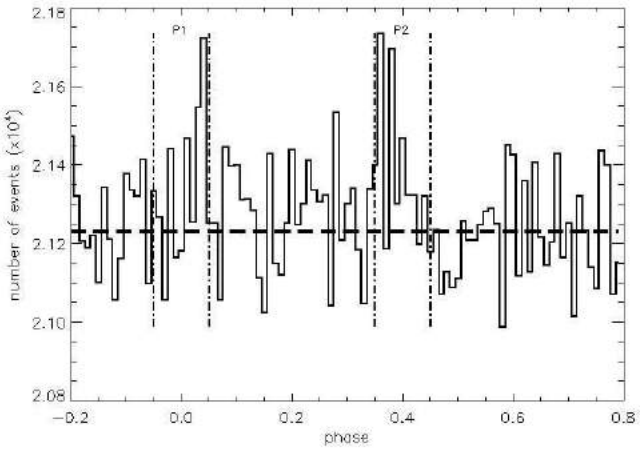

Figure 4. Phasogram of Crab pulsar from HAGAR. Excess is seen at phases marked by P1 and P2.

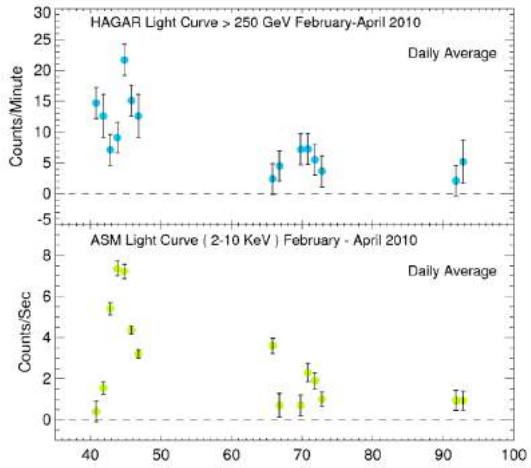

Figure 5. Light curve of Mkn 421 from HAGAR during February-April 2010 (top panel) and corresponding X-ray light curve from ASM onboard RXTE.

radio data from OVRO, optical data from SPOL, X-ray data from Swift and RXTE, high energy gamma ray data from Fermi-LAT and VHE data from HAGAR. Multiwaveband light curves for February 2010 are shown with panels arranged in the order of increasing energy from top to bottom. Flare peaking around 16-17th February is seen in most of the wavebands.

Evolution of Mkn 421 SED was studied during this flaring episode. For this purpose, multiwaveband light curve was divided into four states, pre-flare (13-15 February), moderate flare (16 February), TeV flare (17 February) and post flare (18-19 February) state. SEDs were generated for these four states and fitted with Synchrotron Self Compton model. One zone SSC model developed by Krawczynski et al. [21] was used for this purpose. SED during TeV flare state is shown in Fig.6 along with the one zone SSC fit. For all the states one zone SSC model seems to fit data well. Model parameters for all four states are listed in Table 1. We tried to explain this flaring episode in terms of passing shock and details are given in [22].

Work on longterm data of Mkn 421 covering seven years (2009-2015) is underway. Lightcurve from HAGAR data is shown in Fig.7. Multiwaveband light curves and SEDs are being studied [23].

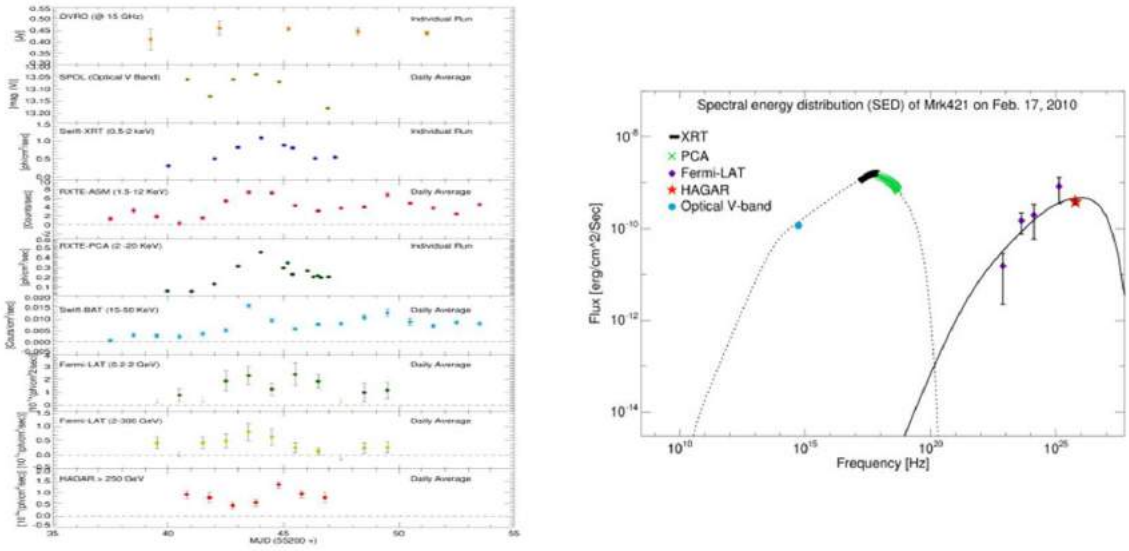

Figure 6. Left panel : Multiwaveband light curve of Mkn 421 during February 2010, Right panel : Multiwaveband SED of Mkn 421 during flare detected by HAGAR on 17th February 2010.

Table 1. Parameters for single zone SSC fit to Mkn 421 SEDs.

State	Magnetic field (G)	Doppler factor δ	log E_{min} (eV)	log E_{max} (eV)	log E_{break} (eV)	p1	p2	U_e $[10^{-3}]$ (erg/cc)	$\eta = U_e/U_B$
State1	0.026	19.5	9.6	12.1	11.3	2.4	4.3	0.9	33.46
State2	0.029	22.0	8.0	12.1	11.4	2.2	3.9	1.4	41.83
State3	0.029	21.0	9.4	12.1	11.45	2.2	4.1	1.0	29.88
State4	0.028	21.0	9.1	12.1	11.45	2.3	4.1	8.5	27.24

3.5.4 *Mkn 501*

Another Blazar observed extensively with HAGAR is Mkn 501. This is again nearby Blazar (z=0.034) of HBL type, discovered by Wipple in 1996. It is a highly variable source. Data collected by HAGAR in years 2010 and 2011 are analysed. Source was detected 5σ significance level during April-May 2011 with flux level of 1.5 crab units. Multiwaveband light curve is generated and SEDs are fitted with SSC model. These SEDs could not be fitted with one zone SSC model. So additional zone was introduced and two zone SSC model was found to give satisfactory fit as shown in Fig.8. According to this model, there are two emission zones, inner and outer one. Radius of inner zone corresponds to variability time scale of 7 hours and outer zone to 48 hours. Further details are given in [24].

3.5.5 *Other Blazars*

We have observed some more blazars using HAGAR including 1ES1426+428, 1ES1218+304 and 3C454.3. First two Blazars are detected by MAGIC experiment, but at much lower flux level compared to Mkn 421 and Mkn 501. HAGAR sensitivity being inferior to VERITAS and MAGIC, these Blazars were not detected with HAGAR with good statistical significance. 3C454.3 is not detected by any VHE experiment probably because of its high redshift (z=0.859). It was observed by HAGAR during detection of flare by Fermi-LAT in year 2009. There is no statistically significant detection of gamma ray signal from HAGAR data and upper limits on flux were estimated for all these source. Details of these results are given in [25].

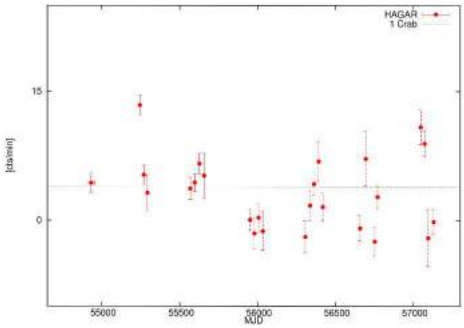

Figure 7. Lightcurve of Mkn 421 from HAGAR during 2009-2015.

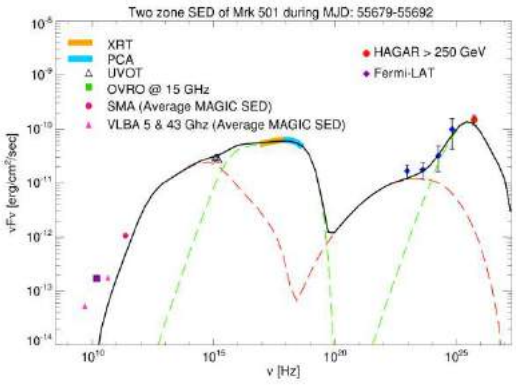

Figure 8. Multiwaveband SED of Mkn 501 fitted with two zone SSC model.

4. Future prospects

After successful installation and operation of HAGAR at Hanle, HiGRO collaboration is entering more ambitious second phase of experiments, i.e. MACE telescope. Installation of MACE is at advanced stage at Hanle and first light is expected by 2017 [14]. Also there are plans of participation in next generation observatory, Cherenkov Telescope Array, an international collaboration involving 1200 scientists/engineers from 31 countries [26, 27].

References

[1] http://tevcat.uchicago.edu/
[2] F. Aharonian et al., A&A **464**, 235 (2007).
[3] A. A. Abdo et al., ApJ **708**, 1254 (2010).
[4] R. Buehler et al., ApJ **749**, 26 (2012).
[5] E. Aliu et al., Science **334**, 69 (2011).
[6] S. Ansoldi et al., A&A **585**, A133 (2016).
[7] C. Stegman, for HESS collaboration, presentation at TeVPA-2014, June 2014, Amsterdam.
[8] J. Albert et al., Science **312**, 1771 (2006).
[9] I. F. Mirabel, Science **312**, 1759 (2006).
[10] F. Aharonian et al., ApJ **664**, L71 (2007).
[11] J. Albert et al., ApJ **669**, 862 (2007).
[12] F. Aharonian et al., Nature **440**, 1018 (2006).
[13] A. Abramowski et al., A&A **550**, A4 (2013).
[14] K. K. Yadav, these proceedings.
[15] K. S. Gothe et al., Experimental Astronomy **35**, 489 (2013).

[16] V. R. Chitnis et al., 32nd International Cosmic Ray Conference, Beijing, China, **9**, 166 (2011).
[17] D. Heck et al., Report FZKA6019, Forschungszentrum Karlsruhe GmbH, Karlsruhe (1998).
[18] L. Saha et al., Astroparticle Physics **42**, 33 (2013).
[19] B. B. Singh et al., paper presented at 33rd ASI meeting at NCRA-Pune during 17-20 February 2015.
[20] B. B. Singh et al., 32nd International Cosmic Ray Conference, Beijing, China, **7**, 87 (2011).
[21] H. Krawczynski et al., ApJ **601**, 151 (2004).
[22] A. Shukla et al., A&A **541**, id.A140 (2012).
[23] A. Sinha et al. To appear in A&A (2016).
[24] A. shukla et al., ApJ **798**, id.2 (2015).
[25] P. Hazarika et al., these proceedings.
[26] https://portal.cta-observatory.org/Pages/Home.aspx
[27] B. S. Acharya et al., Astroparticle Physics **43**, 3 (2013).